Geoscientific
Model Development
Discussions

Supplement of

Upscaling with the dynamic two-layer classification concept (D2C): TreeMig-2L, an efficient implementation of the forest-landscape model TreeMig

J. E. M. S. Nabel

Correspondence to: J. E. M. S. Nabel (julia.nabel@mpimet.mpg.de, jemsnabel@gmail.com)

A. Additional details on the implementation of TreeMig-2L

A.1. Data structures

The architecture of TreeMig-2L comprises different data structures (Fig. A.1 and Fig. 2, main text). Processes on the two-dimensional layer require information on the spatial location of a grid cell relative to other grid cells. State variables required for these spatial processes are therefore stored in an array data structure. Processes on the non-spatial layer do not require information on the spatial location of a grid cell relative to other grid cells. Furthermore, the number of elements on the non-spatial layer, as opposed to the number of grid cells, is not pre-determined by the considered simulation area but emerges during the simulation. Therefore, the elements on the non-spatial layer need to be stored in a dynamic data structure. The dynamic data structure used for TreeMig-2L is a doubly linked list. A doubly linked list is a data structure in which each element is connected to two other elements of the list, its predecessor and its successor. Therefore, such a list can dynamically grow or shrink only changing local information instead of global information and allows for efficient traversal. The dynamic character of the non-spatial layer, i.e. splitting and merging of its elements induces an overhead required for the maintenance of its elements. To pre-constrain this overhead, multiple small lists are used instead of one large list. This enables efficient splitting and merging operations which only apply to a single list, but not to the whole non-spatial layer. In particular the comparison of elements would induce a larger overhead if all elements would be compared to all other elements, instead of restricting comparison to the other elements in one of the small lists. To pre-define which element is stored in which list, the fact is used that for grid cells to be similar not only species' compositions need to satisfy the given similarity criteria but also bioclimatic influences need to be comparable. As opposed to species' compositions which develop during runtime, bioclimate drivers are an input to TreeMig. Information about the bioclimate drivers can therefore be used in advance to pre-structure a simulation area. In this pre-structuring bioclimate types are derived from the bioclimate drivers according to a given set of bioclimate bins (see Section A.2. and Section 3.1.3, main text). Each of the derived bioclimate types is associated with one list (Fig. A.1). Because the number of the bioclimate types is known in advance, information about the bioclimate types can be stored in a one dimensional array structure.

The different data structures, i.e. the array for the two-dimensional layer, the one-dimensional array for bioclimate types and the linked lists for elements on the non-spatial layer, are asymmetrically connected (Fig. A.1). Each bioclimate type has a pointer – a data type allowing direct access – to the first element in its list. Furthermore, each cell of the two-dimensional layer has a pointer to the element with which it is currently associated, to allow for a direct and thus fast exchange of the status information.
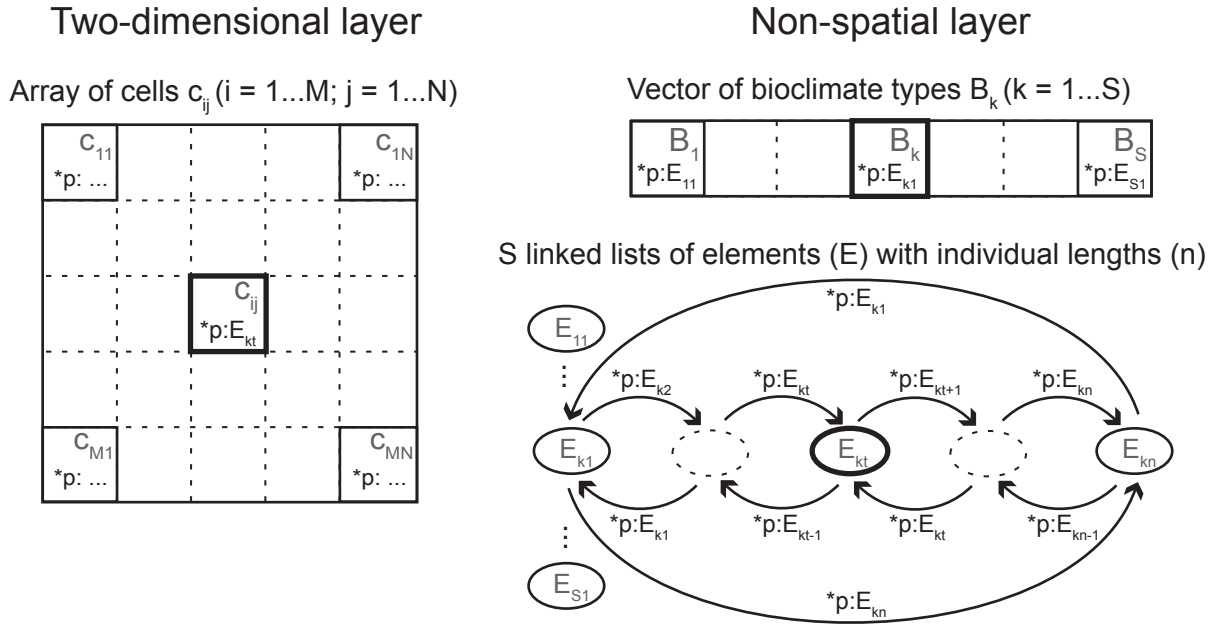

Fig. A.1: Data structures used in TreeMig-2L and their connections. State variables required for processes simulated on the two-dimensional layer (see Fig. 2, main text) are kept in cells stored in an M x N array structure (size according to the simulation area). The non-spatial layer comprises different data structures: a vector of bioclimate types (length S) and associated linked lists for each of these types containing the actual elements on the non-spatial layer. The bioclimate types are derived in a pre-processing (see Section A.2. and Section 3.1.3, main text). Connections between the different data structures are asymmetric and defined with pointers. A pointer is a data structures holding the memory location of another data structure and therefore allowing direct access. Each cell (c_{ij}) on the two-dimensional layer holds a pointer (*p:E_{kt}) to the element on the non-spatial layer it is currently associated with (E_{kt}). Each bioclimate type (B_k) holds a pointer (*p:E_{k1}) to the first element of its associated list (E_{k1}). Elements stored in the linked lists do not contain pointers to their associated cells because the number of associated cells can change during simulation time. For explanatory reasons, list k is depicted containing several elements and c_{ij} points to element E_{kt}. However, a list can also consist of only one element which then points to itself.

A.2. Pre-structuring of a simulation area

A simulated area is pre-structured to bioclimate types according to the bioclimate drivers, i.e. grid cells are classified according to their bioclimate drivers. The underlying idea of the pre-structuring is that the spatial correlation in the bioclimate among cells of the simulation area is rather persistent (see Nabel et al., 2014). Due to this correlation, two cells having similar bioclimate drivers for a certain time span have a good chance to have similar bioclimate drivers beyond this time span (see the examples in Fig. C.5 and C.6). With this in mind, similarity of cells is not tested for each point in the entire time span covered by the bioclimate driver, but only for the averages of pre-defined 'supporting periods' (see Fig. A.2 for an example). For each of the supporting periods and for each of the bioclimate drivers one average per cell is calculated (Fig. A.2a). For each bioclimate driver, the according averages are then classified according to pre-defined bioclimate bins (Fig. A.2b). Each actually occurring set of classes defines one bioclimate type (Fig. A.2c). The number of possible bioclimate types will therefore be influenced by the number of supporting periods and the number of bioclimate bins (see for example Fig. C.4). A small number of supporting periods and of bioclimate bins will lead to a coarser discretisation to bioclimate types, whilst more periods and more bins will lead to a finer discretisation. After associating each cell with one bioclimate type, the bioclimate influence for this type is calculated as the average of all associated cells for each point in time and each bioclimate variable (e.g. Fig. A.2c).
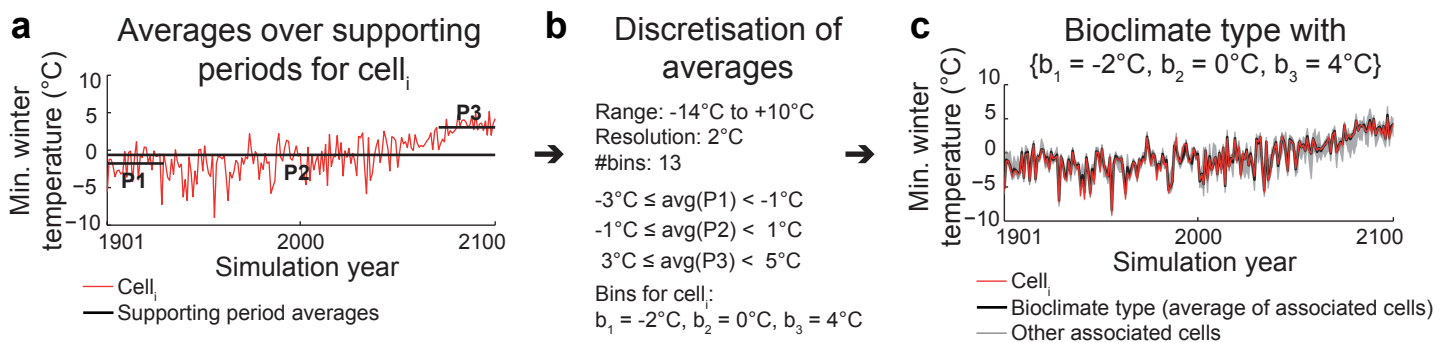

Fig. A.2: Visualisation of the pre-structuring to bioclimate types on the example of the minimum winter temperature (Min. winter temperature), one of TreeMig's three bioclimate drivers. (Panel a) For each of the supporting periods (here P1-P3) the minimum winter temperature driving $cell_i$ is averaged. (Panel b) In the example the minimum winter temperature in the simulation area is assumed to range from $-14\,°C$ to $+10\,°C$ discretised with a resolution of $2\,°C$ into 13 bins (as e.g. done for the set E3 of bioclimate bins in Table 2, main text). The averages of the supporting periods P1-P3 for $cell_i$ are clustered according to these bins. (Panel c) All cells with supporting periods clustered into the same bins are associated with the same bioclimate type and the bioclimate influence for a bioclimate type is calculated as the average of all associated cells for each point in time.

Bioclimate types receive a unique ID and are stored in a NetCDF file (Unidata - `http://www.unidata.ucar.edu/software/netcdf/`) used in two-layer simulations to read the bioclimate driver. Depending on the ratio of the number of bioclimate types to the number of cells in the simulation area, this NetCDF file is much smaller than the original NetCDF file which stores bioclimate input data for each single cell (e.g. the NetCDF file for the E1 version of the application scenario A1, having a 1:33 ratio of bioclimate types to cells, has a size of 9MB instead of the 400MB required for the original file).

Most TreeMig simulations start with an initialisation phase from bare ground with a reduced number of simulated processes, in particular without simulating seed dispersal (cf. Lischke et al., 2006; Nabel et al., 2013). Thus, the linked list of each bioclimate type (see Fig. A.1) will contain exactly one element over the whole time span of this initialisation phase. Simulations not starting from bare-ground but with given species' abundances would require an additional pre-processing step, introducing appropriate numbers of elements according to the different species' abundances occurring for the different bioclimate types.

A.3. Execution sequence in TreeMig-2L

The implementation of TreeMig-2L is based on TreeMig-Netcdf 2.0 (Nabel et al., 2014) and the gross of the program structure was adopted from there. However, besides the changes in data structures (see Section A.1) also some changes in the execution sequence were required (see Fig. A.3).
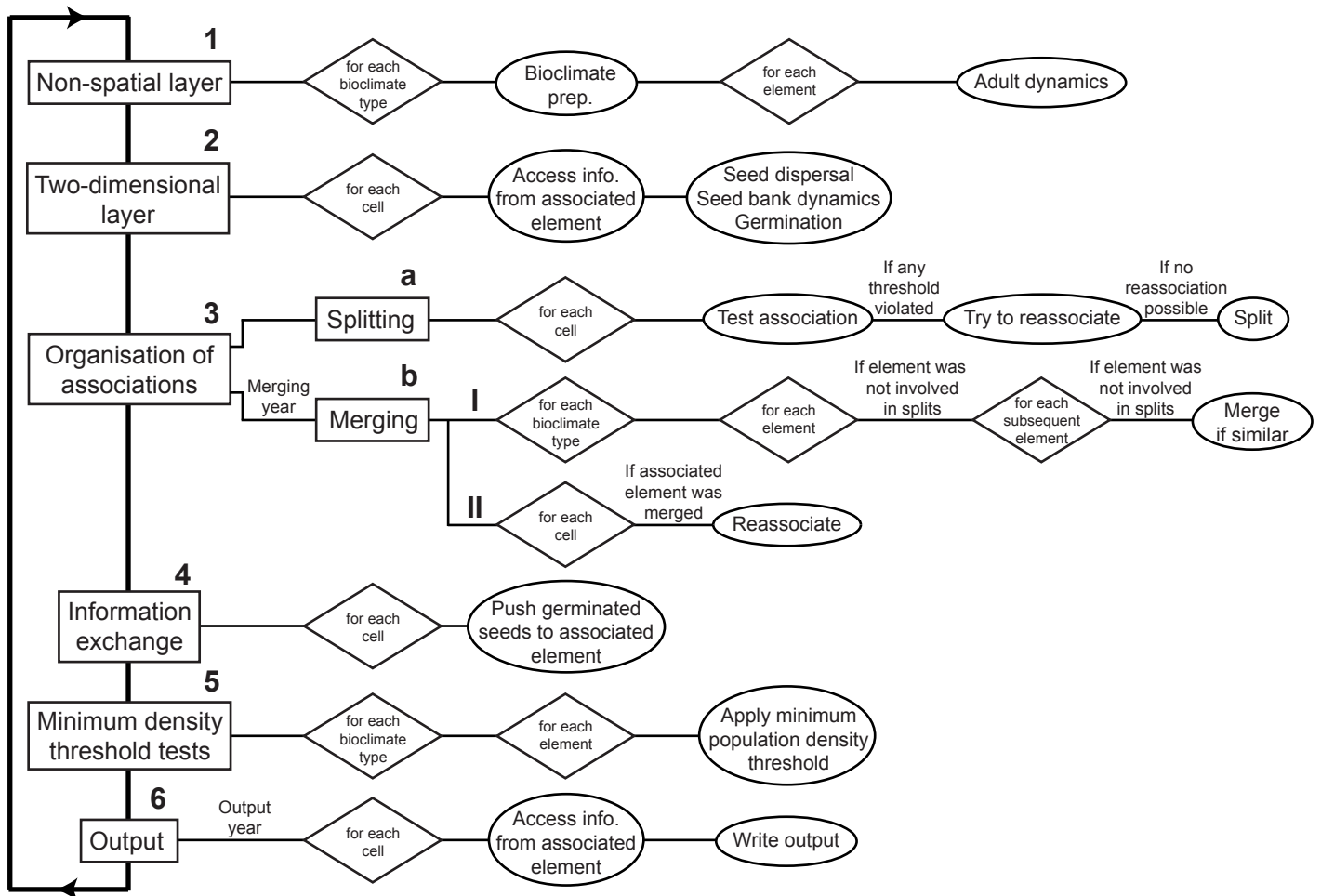

Fig. A.3: Execution sequence per time step in TreeMig-2L. (1) Each time step begins with the execution of the processes simulated on the non-spatial layer. For each bioclimate type the current bioclimate driver is read (or drawn in case of extrapolations), species-specific influences are derived and they are used for simulations of adult dynamics (described in detail in Lischke et al., 2006) in each element of the linked list of the bioclimate type. (2) Subsequently, processes simulated on the two-dimensional layer are conducted. Since each cell has a pointer to the element it is currently associated with (Fig. A.1 and Fig. 2, main text), it can access required information for seed dispersal and germination. (3a) Seeds germinated in the current time step can necessitate splitting of elements. Therefore, current associations are tested for each cell and if any threshold on the density of germinated seeds for any tracked species is violated the association is no longer valid. In case that the current associated element already had splits in the current time step, the cell can be reassociated to an element from a previous split if the thresholds on the germinated seed densities are met. If not, the current element is split up and the cell is associated with the new element. (3b) Merging is only done after a pre-defined number of time steps. (3b.I) In a merging year, all elements in the list of a bioclimate type are compared and similar elements are merged. Two elements are thereby only merged if none of them was involved in any splits in this time step. (3b.II) After merging was conducted, cells whose associated elements were merged need to be reassociated. (4) After the associations are reorganised, cells can push the number of seeds germinated in this time step to their associated elements. (5) To prevent infinitesimal values, the population densities per height class kept in each element on the non-spatial layer are tested for adherence of a pre-specified minimum density threshold (see Nabel et al., 2013). Values falling below the threshold are added to lower height classes or removed, in case of the lowest height class. (6) The output of TreeMig-2L is written at the end of each time step for each cell, provided the current time step is an output year.

B. Additional information about the application scenarios

For this study, TreeMig-2L simulations were conducted for two application scenarios with different simulation settings which are briefly characterised in Table 1 in the main text. The location of the simulation areas in Switzerland are depicted in Fig. 3 in the main text. In this supplementary material, additional information for the two application scenarios is provided.

As described in Section 3.1.1 in the main text, TreeMig simulations require time series of three annual bioclimate drivers. The bioclimate influences used for the two application scenarios were derived from monthly averaged temperatures and monthly precipitation sums from different SRESA1B (Nakicenovic et al., 2000) scenario projections with a program based on ForClim-E (Bugmann and Cramer, 1998; Lischke et al., 2006) – for more details on the actual climate time series see below (B.1 and B.2). Bioclimate types for both application scenarios were derived with the same set of bioclimate bins (see Table 2, main text) using three sampling periods: (1) the first 30 years (A1: 1961-1991; A2: 1901-1931), (2) the whole time span (A1: 1961-2100; A2: 1901-2100) and (3) the last 30 years (both: 2071-2100). Because the simulated time spans of both application scenarios exceeded the available bioclimate data, a stochastic method was used to extrapolate the bioclimate driver (see B.3 for further information). Simulations with both scenarios started in 1400 with an initialisation phase lasting 400 years. In this initialisation phase only a restricted set of processes was simulated assuming that saplings of all species are available in all elements (with one restriction in application scenario A2, see B.2 below) instead of simulating seed production, dispersal and germination (cf. Lischke et al., 2006; Nabel et al., 2013).

The two-layer simulations discussed in the main text all applied the same set of splitting and merging thresholds. These thresholds were defined on a unit area, the so-called patch area (cf. Bugmann, 1994), because TreeMig's state variables represent means of Poisson distributions of tree densities per species and height class on this unit area (Lischke et al., 1998, 2006). For the splitting of elements two thresholds were used, namely 0.005 and 0.5 germinated seeds per patch area. These two thresholds were used to divide the number of germinated seeds in three bins: absence of germinated seeds, scattered germinates seeds and more than one seed on every second patch. Elements on the non-spatial area were split if the germinated seeds of any of the species tracked in the application scenario fell on different sides of these thresholds for at least two associated cells. Merging was considered every 100 simulation years and elements were merged if the difference in the densities for all occurring species and height classes did not exceed a height-specific similarity threshold (50.0, 25.0, 20.0, 15.0, 10.0, 7.5, 5.0, 2.5 individuals per patch for the lowest eight height classes, respectively, and 1.0 for all other height classes).

In addition to the simulations discussed in the main text, some sensitivity tests were conducted with different splitting and merging thresholds and a different merging interval. Results for these sensitivity tests are shown and discussed in Section C. For A1 and A2, tests were conducted only considering presence and absence of germinated seeds for splitting, i.e. with only one splitting threshold (0.05). For A2, additional tests with a larger set of splitting thresholds were conducted (0.0005, 0.005, 0.05, 0.5, 5.0 and 50.0 germinated seeds per patch area). For both application scenarios, a merging interval of 10 simulation years and merging conditional on smaller differences for the densities in the height classes were tested (5.0 individuals per patch area for the first seven height classes and 1.0 individuals for all other height classes).

All simulations were conducted without disturbances (other than climatically caused) and the boundaries of the simulation areas were assumed to be absorbing, i.e. seeds dispersed beyond the boundaries were lost. In both application scenarios a minimum population density threshold (see Nabel et al., 2013) of one individual per grid-cell was applied.

B.1. Application scenario A1

Application scenario A1 has already been used in a previous study to test the performance of a preliminary version of TreeMig-2L in simulations without dynamic associations between the layers (Nabel and Lischke, 2013). The bioclimate influences used for A1 simulations were derived from an SRESA1B scenario simulation calculated with RCA3 (1961-2100 – Kjellström et al., 2005) and downscaled to 200 m cell side length based on a grid of MeteoSwiss weather stations interpolated with daymet (Thornton et al., 1997). In addition to the monthly climate data, static data for the simulation area on slope, aspect and water holding capacity was used to calculate the bioclimate drivers. Slope and aspect were averaged from the 25 m digital elevation model of the Swiss Federal Office of Topography (DHM25 (c)1994 Bundesamt für Landestopographie). The water holding capacity was derived from data on water retention potential and soil wetness found in the Swiss soil suitability map (Frei et al., 1980) by means of a linear regression based on soil profiles at test sites according to (Löffler and Lischke, 2001).

A1 simulations were conducted for 1100 years (1400-2500) and simulated for 31 species occurring in Switzerland. These species were parameterised for previous TreeMig applications. Parameters for 30 species were taken from Lischke et al. (2006) altered according to the findings in Rickebusch et al. (2007), namely *Abies alba, Larix decidua, Picea abies, Pinus cembra, P. montana, P. sylvestris, Taxus baccata, Acer campestre, A. platanoides, A. pseudoplatanus, Alnus glutinosa, A. incana, A. viridis, Betula pendula, Carpinus betulus, Castanea sativa, Corylus avellana, Fagus sylvatica, Fraxinus excelsior, Populus nigra, P. tremula, Quercus petraea, Q. pubescens, Q. robur, Salix alba, Sorbus aucuparia, Tilia cordata, T. platyphyllos* and *Ulmus scabra.* Parameters for the 31th species *Ostrya carpinifolia* were taken from Nabel et al. (2012).

For the A1 simulations with two layers discussed in the main text, four species were used to decide if an element on the non-spatial layer needs to be split: *Q. pubescens, O. carpinifolia, L. decidua* and *P. silvestris*. These four species were selected as

tracked species because of their high drought tolerance indices in TreeMig. With increasing drought severity (and temperature), these species are expected to increase their distributions. In addition to simulations with these four tracked species, simulations with two tracked species (*P. silvestris* and *Q. pubescens*) and simulations with six tracked species (the four species already listed and the two species most abundant in the simulation area *P. abies* and *F. sylvatica*) were conducted to assess the sensitivity of the simulation results to the choice of tracked species.

B.2. Application scenario A2

Application scenario A2 was used in previous studies to investigate the influence of interannual bioclimate variability on the northwards migration of *O. carpinifolia* (Nabel et al., 2012, 2013). Bioclimate influences were derived from CRU data (1901-2000 – Mitchell et al., 2003) followed by an SRESA1B scenario simulation calculated with CLM (2001-2100 – Lautenschlager et al., 2009 which was downscaled to 30″ with WorldClim data (Hijmans et al., 2005) and projected to 1 km^2 with FIMEX-0.28 (Klein, 2012). In addition to the monthly climate data, static data for the simulation area on slope, aspect and water holding capacity was used (see supplementary material to Nabel et al. (2013) for more details).

A2 simulations were conducted for 1600 years (1400-3000) and in addition to *O. carpinifolia* 20 other species were simulated: *A. alba*, *L. decidua*, *P. abies*, *P. cembra*, *P. sylvestris*, *Taxus baccata*, *A. platanoides*, *A. pseudoplatanus*, *A. incana*, *B. pendula*, *C. betulus*, *C. sativa*, *F. sylvatica*, *F. excelsior*, *P. tremula*, *Q. petraea*, *Q. pubescens*, *S. aucuparia*, *T. cordata*, *T. platyphyllos* and *U. scabra*.

As opposed to all other species, saplings of *O. carpinifolia* were restricted to the southern part of the transect up to the 65th transect km north in the initialisation phase (1400-1800) of the A2 simulations. From the simulation year 1800 on the northwards migration of *O. carpinifolia* was simulated. For the A2 simulations discussed in the main text the optimistic end of the range of plausible species parameters for *O. carpinifolia* (see Nabel et al., 2012) was used because the migration through the transect was not restricted for this parameter set in a previous simulation study (Nabel et al., 2013).

B.3. Extrapolation of the bioclimate time series

To extrapolate the available bioclimate time series for the entire simulated time spans a stochastic method was used. Nabel et al. (2014) recommended that a method used to extrapolate time series for spatially explicit simulations should account for the spatial correlation of climatic fluctuations in the extrapolated data. Therefore, the simple method of drawing complete bioclimate maps from a set of base years used in Nabel et al. (2014) was also used in this study. For extrapolation of past simulation years the first 30 years of the input data for each of the two application scenarios (A1: 1961-1990 and A2: 1901-1930) were used to derive a set of detrended base years (see supplementary material to Nabel et al. (2013) for more information on the detrending). For extrapolations of future simulation years the last 30 years (2071-2100 for both application scenarios) were used to derive a second set of detrended base years.

In the pre-structuring of the simulation area, required for two-layer simulations with TreeMig-2L, the bioclimate information is transferred from the cell level to the bioclimate types. This does not affect the applicability of the extrapolation method: The only difference to simulations on one layer is that in each year a bioclimate map for all bioclimate types is drawn instead of a bioclimate map for all single cells.

C. Additional information on the pre-structuring, the influence of the bioclimate and conducted sensitivity tests

C.1. Pre-structuring of the simulation areas

The number of cells associated with the bioclimate types is influenced by the number of supporting periods, the number of bioclimate bins and the heterogeneity of the simulation area. Bioclimate types representing bins with frequent occurrences in the simulation area will end up with more cells than bioclimate types representing rare bioclimatic conditions. The distribution of cells to bioclimate types for the two application scenarios (A1 and A2) and the three sets of bioclimate bins (E1-E3) reflect this (see Fig. C.4, Fig. C.5 and Fig. C.6).

In the pre-structuring of the simulation area, each bioclimate type receives a unique ID (see Section A.2). This ID is theoretically arbitrary, however, the underlying algorithm in TreeMig-2L assigns the IDs in a specific order. When searching for similarities among cells, one supporting period after the other is processed and the three bioclimate variables are considered in the order: (1) sum of daily mean temperatures above $5.5\,^\circ C$ (DDsum$_{>5.5\,^\circ C}$), (2) minimum winter temperature, and (3) drought index; each increasing from the smallest to the largest occurring value. Thus, the IDs of the bioclimate types are monotonous increasing with the DDsum$_{>5.5\,^\circ C}$ of the first supporting period and allow some insights into the distribution of IDs for the DDsum$_{>5.5\,^\circ C}$ in the simulation area (Fig. C.4 and Fig. C.7). For example, the tendency for bioclimate types with most associated cells to have IDs in the middle of the ID-ranges, i.e. DDsum$_{>5.5\,^\circ C}$ values in the moderate range of the simulation area.
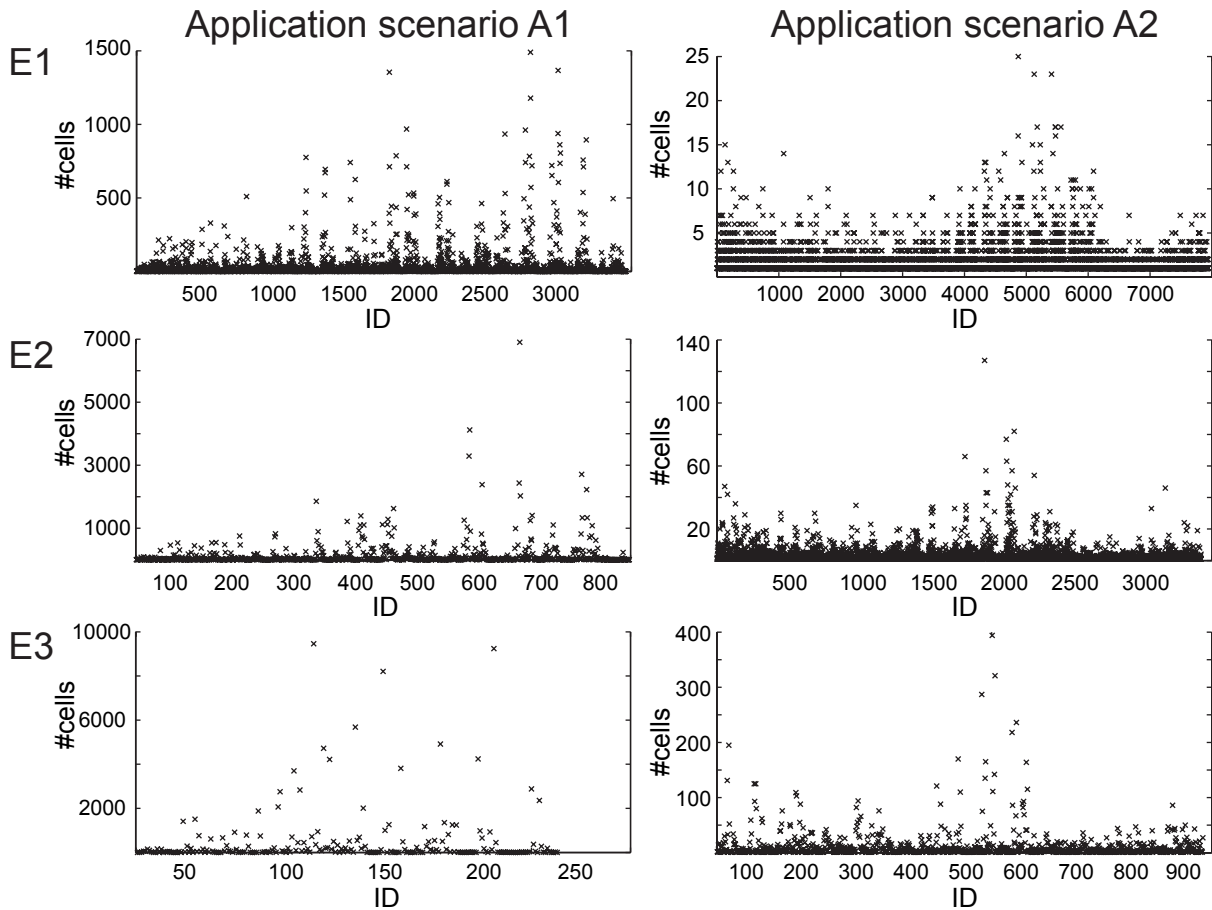

Fig. C.4: Number of cells associated with all three sets of bioclimate types (E1-E3) for the simulation areas of application scenario A1 and A2. The number of cells per bioclimate type varies strongly among the three sets and the simulation areas (note the different scales).

A finer discretisation by means of smaller bioclimate bins in the pre-structuring of the simulation area tends to lead to a smaller number of cells associated with the bioclimate types (Fig. C.4) and to smaller deviations between the averaged bioclimate and the bioclimate of the single associated cells (Fig. C.5 and Fig. C.6). This is also supported by the differences among the bioclimate variables. For all sets of bioclimate bins the DDsum$_{>5.5\,^\circ C}$ was discretised into more bins (see Table 2, main text) leading to smaller maximum differences between DDsum$_{>5.5\,^\circ C}$ time series of bioclimate types and their associated cells than for the other variables (Fig. C.5 and Fig. C.6).
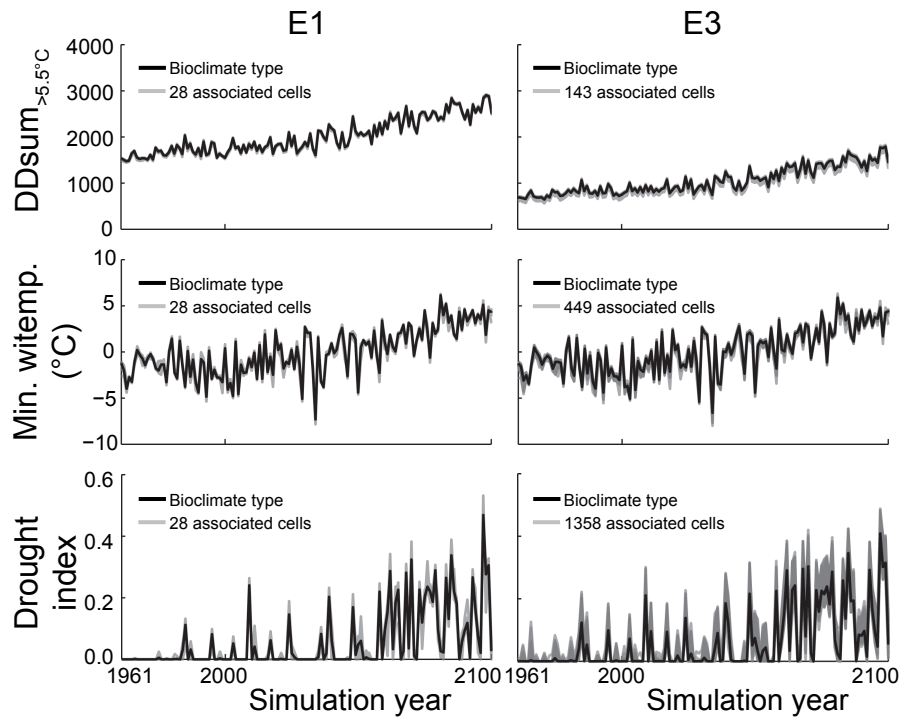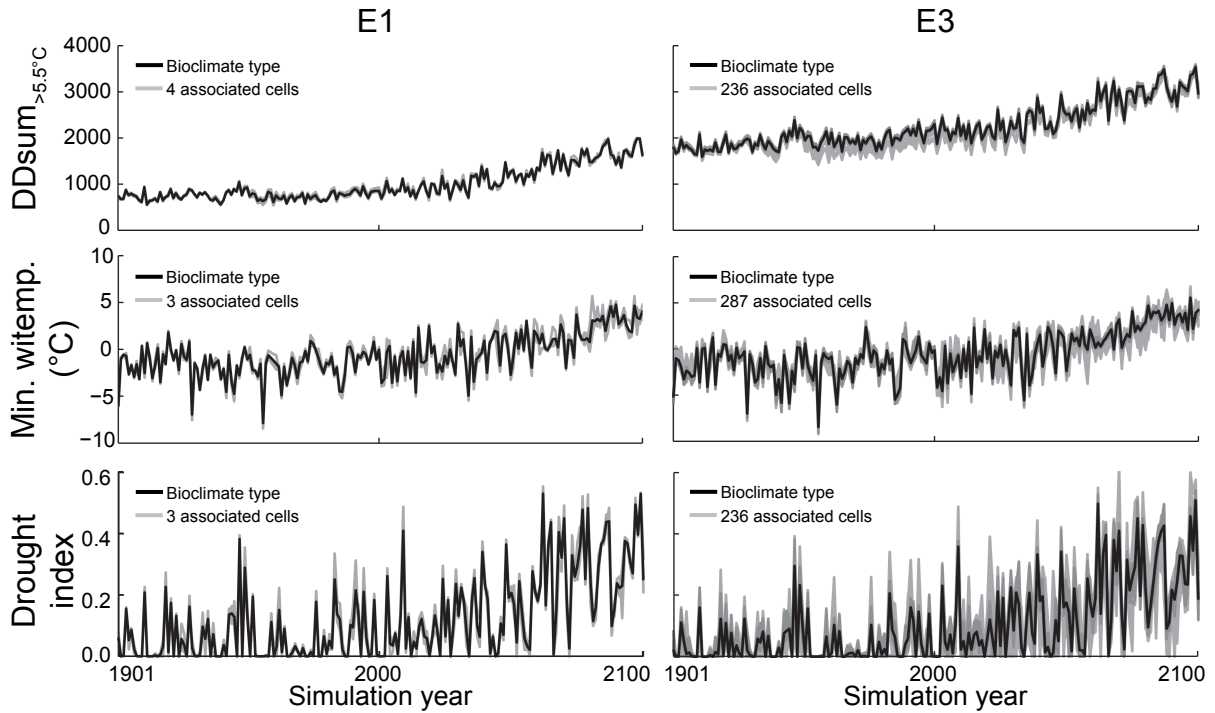
Fig. C.5: Average bioclimate for the bioclimate types (black lines) and for their associated cells (grey half-transparent lines). Depicted are those bioclimate types which averages deviated the most from one of their associated cells for pre-structurings of the simulation area of application scenario A1 with the fine (E1) and the coarse (E3) bioclimate bins for each of TreeMig's bioclimate drivers (DDsum$_{>5.5\,°C}$: Sum of daily mean temperatures above 5.5 °C; Min. witemp.: Minimum winter temperature; and the drought index).

Fig. C.6: Average bioclimate for the bioclimate types (black lines) and for their associated cells (grey half-transparent lines). Depicted are those bioclimate types which averages deviate the most from one of their associated cells for pre-structurings of the simulation area of application scenario A2 with the finer (E1) and the coarse (E3) bioclimate bins for each of TreeMig's bioclimate drivers (DDsum$_{>5.5\,°C}$: Sum of daily mean temperatures above 5.5 °C; Min. witemp.: Minimum winter temperature; and the drought index).
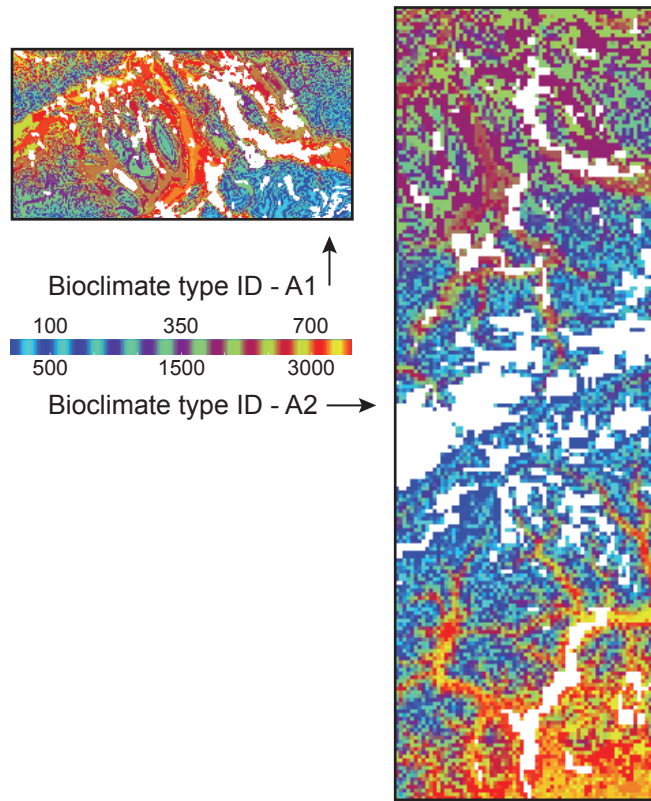
Fig. C.7: Distribution of the IDs of the bioclimate types in space for the two application scenarios A1 and A2. Depicted are bioclimate type IDs for the moderate set of bioclimate bins (E2 – see Table 2, main text). Although the IDs of the bioclimate types are theoretically arbitrary they allow some insights into the distribution of IDs for the DDsum$_{>5.5\,°C}$, due to the algorithm used to derive the bioclimate types (see text of Section C.1). For both simulation areas close IDs (i.e. IDs with close DDsum$_{>5.5\,°C}$ values) visibly cluster in space, following elevations in the transect area (see Fig.2, main text). ID-maps were created with ncview (Pierce, 2012).

C.2. Influence of interannual bioclimate variability and of changes in the bioclimate over time

To assess the relevance of deviations from 1.0 in the different similarity coefficients (SCs), results from 1L-ORG simulations using different pseudo-random number streams (PRNSs) to extrapolate the bioclimate driver were compared among each other. Since these simulations only differ in the stochastically extrapolated bioclimate (before 1961 for A1, before 1901 for A2, and after 2100 for both application scenarios – see Section B.3) deviation from 1.0 in their SCs (Table C.1 and Fig. C.8) are due to the interannual variability in the bioclimate driver.

Table C.1: The similarity coefficient (SC) was used to compare different output variables among 1L-ORG for simulations applying different pseudo-random number streams (PRNSs) to extrapolate the bioclimate driver. These SCs thus show the influence of the interannual bioclimate variability on the similarity among simulations with otherwise similar conditions. SC means and standard deviations stem from comparisons among simulations with different PRNSs – five for A1 (ten comparisons) and 20 for A2 (190 comparisons).

	Avg. SC (σ)		
	SC_{sum}	SC_{spec}	SC_{OC}
A1	0.95 (0.02)	0.87 (0.04)	–
A2	0.92 (0.03)	0.86 (0.03)	0.79 (0.05)

Inter-comparisons of 1L-ORG simulations led to SC_{spec} (Fig. C.8a) and SC_{sum} (not shown) values close to 1.0 until 2100 for the homogeneous simulation area of application scenario A1. For the more heterogeneous simulation area of application scenario A2 there were small deviations from 1.0 in the SCs (Fig. C.8b and c), which vanished during the time span simulated with a deterministic bioclimate driver (1901-2100). Directly after 2100 the SCs rapidly decreased and quickly stabilised on a lower level for both application scenarios. The lower levels in the SCs after 2100 were mainly due to the larger drought index values and the higher interannual variability in the drought index (see e.g. Fig. C.5 and Fig. C.6) which entail larger fluctuations in the simulated species' abundances.
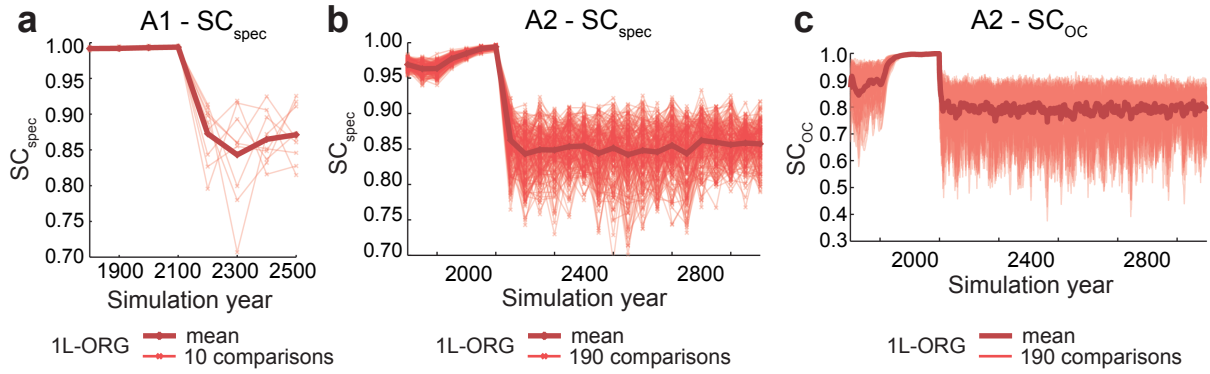
8

Fig. C.8: Temporal development of SC_{spec} for application scenario A1 and A2 and of SC_{OC} for A2 from comparisons among 1L-ORG simulations applying different pseudo-random number streams to extrapolate the bioclimate driver. SC_{spec} values were calculated every 100 years for A1 and every 50 years for A2 simulations; SC_{spec} was calculated for every simulation year. SC_{spec} for A1 stems from comparisons among five simulations (ten comparisons); SCs for A2 stem from comparisons among 20 simulations (190 comparisons). Single simulations and their means are printed half-transparent and bold, respectively. Since the depicted simulations only differ in the stochastically extrapolated bioclimate (before 1961 for A1, before 1901 for A2, and after 2100 for both application scenarios – see Section B.3) deviation from 1.0 in their SCs are due to the interannual variability in the bioclimate driver.

For both application scenarios, and the three different model versions (2L, 1L-PB and 2L-NDA – see Table 3, main text), the development over time of SC_{spec} (Fig. C.9 and Fig. C.10) and SC_{sum} (not shown) were comparable among simulations conducted with all three sets of bioclimate types (E1-E3) and most simulation settings: the SCs decreased in the transient phase of climate change (from around 2000 on) and stabilised after a few centuries. Comparable to 1L-ORG simulations (Fig. C.8) the SCs stabilised on a lower level than before the transient phase, which is again mainly due to the larger drought index values and TreeMigs non-linear reaction on drought indices. Deviations resulting from simulations with the original drought indices and the averaged drought indices have a stronger impact for larger than for smaller drought indices.

Trajectories for SC_{OC} measured for application scenario A2 with 2L-NDA simulations (Fig. C.11) differ from the other trajectories. 2L-NDA simulations were conducted without dynamic associations. Because no splits were conducted *Ostrya carpinifolia* quickly covered the whole simulation area after the spin-up since seeds germinated in any of the cells associated with one element contributed to the average number of germinated seeds in that element. In 1L-ORG simulations, 1L-PB simulations and in 2L simulations with dynamic associations, in contrast, *O. carpinifolia* was initially absent in the northern parts of the transect and only slowly migrated through the transect (Fig. C.12). Therefore, SC_{OC} is much smaller for 2L-NDA simulations than for 2L simulations (maximum differences in the SC of more than 0.3 – Fig. C.11). Because 2L-NDA simulations were conducted without dynamic associations they mainly reflect the changes in the bioclimate over time. In application scenario A2, the bioclimate driver was deterministic from 1901-2100 (see Section B) and a changing climate following the SRESA1B scenario was simulated. After 2000 the temperatures in the southern part of the transect got more and more favourable for *O. carpinifolia* leading to an increase in the biomass of *O. carpinifolia* by the year 2025 for simulations with all simulation settings (Fig. C.12). Because the SC is calculated as the ratio of differences compared to similarities over all cells of a simulation area (see Eq. 1, main text) an increase of the abundances in the south for all simulation settings and stable abundances in the north led to a rapid increase in SC_{OC} for 2L-NDA simulations (Fig. C.11, Fig. C.12). However, after only some decades the bioclimate in the north of the transect also got warm enough to allow for an increase in the biomass of *O. carpinifolia* in 2L-NDA simulations (Fig. C.12). This led to a sharp decrease in SC_{OC} because now the difference in biomass amounts of *O. carpinifolia* in the north of the transect compared to 1L-ORG simulations increased (Fig. C.11). After 2100 SC_{OC} stayed on a stable level for some centuries and started to slowly increase again by the time *O. carpinifolia* started to also spread on the northern side of the Alps in 1L-ORG simulations (Fig. C.11, Fig. C.12).
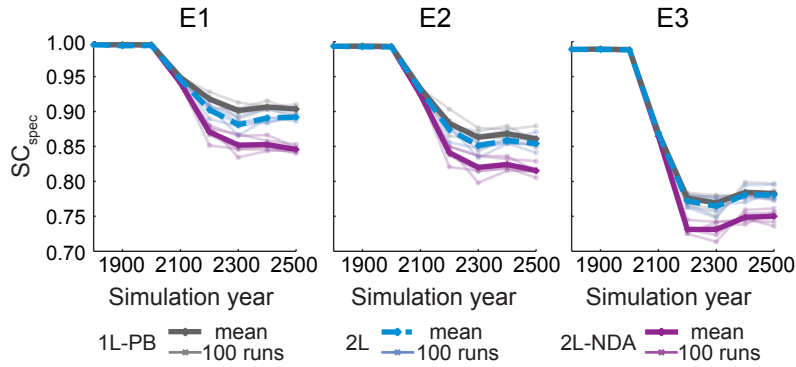
9

Fig. C.9: Temporal development of SC_{spec} for application scenario A1 from comparisons of 1L-ORG simulations to simulations with all three sets of bioclimate types (E1-E3). SC_{spec} values were calculated every 100 years for two-layer simulations with and without dynamic associations (2L and 2L-NDA, respectively) and simulations on one layer but with the bioclimate of the associated bioclimate types (1L-PB). For each setting five repetitions were compared, which were simulated using different pseudo-random number streams to extrapolate the bioclimate driver before 1961 and after 2100. Single simulations and their means are printed half-transparent and bold, respectively.
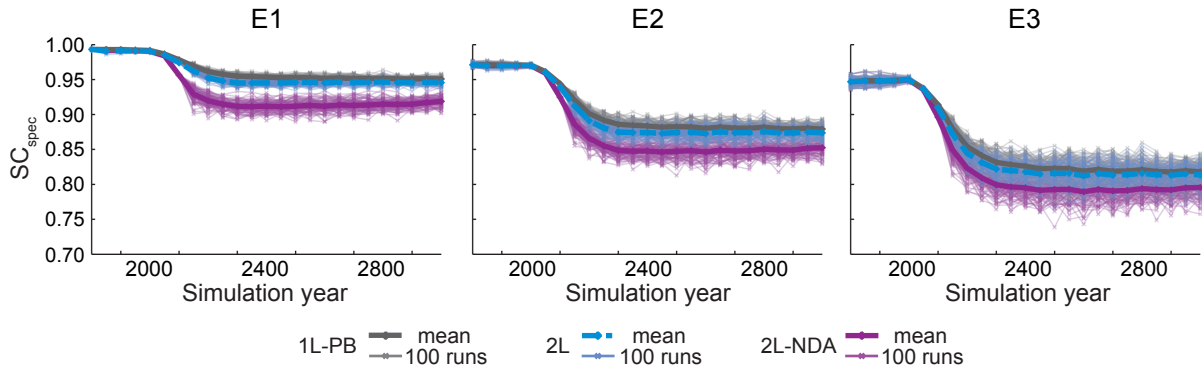

Fig. C.10: Temporal development of SC_{spec} for application scenario A2 from comparisons of 1L-ORG simulations to simulations with all three sets of bioclimate types (E1-E3). SC_{spec} values were calculated every 50 years for two-layer simulations with and without dynamic associations (2L and 2L-NDA, respectively) and simulations on one layer but with the bioclimate of the associated bioclimate types (1L-PB). For each setting 100 repetitions were compared, which were simulated using different pseudo-random number streams to extrapolate the bioclimate driver before 1901 and after 2100. Single simulations and their means are printed half-transparent and bold, respectively.
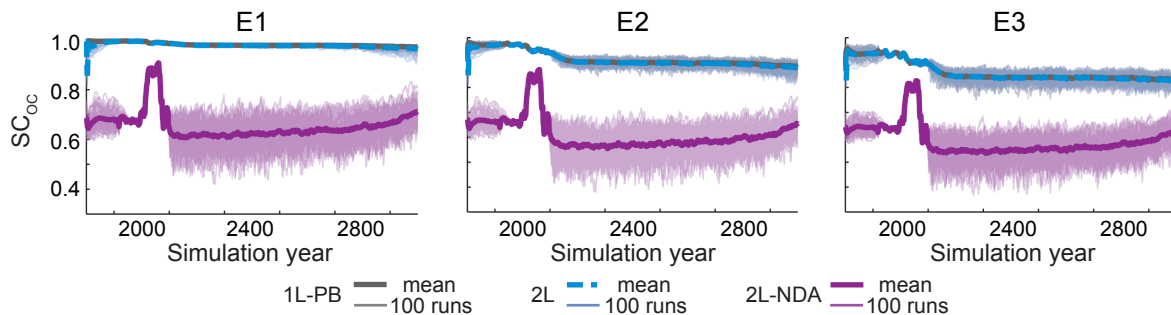

Fig. C.11: Temporal development of SC_{OC} comparing simulations of application scenario A2. Depicted SC_{OC} values stem from comparisons of 1L-ORG simulations to simulations with all three sets of bioclimate types (E1-E3). Simulations were conducted with two-layers with and without dynamic associations (2L and 2L-NDA, respectively) and with one layer but with the bioclimate of the associated bioclimate types (1L-PB). For each setting 100 repetitions were compared, which were simulated using different pseudo-random number streams to extrapolate the bioclimate driver before 1901 and after 2100. Single simulations and their means are printed half-transparent and bold, respectively.
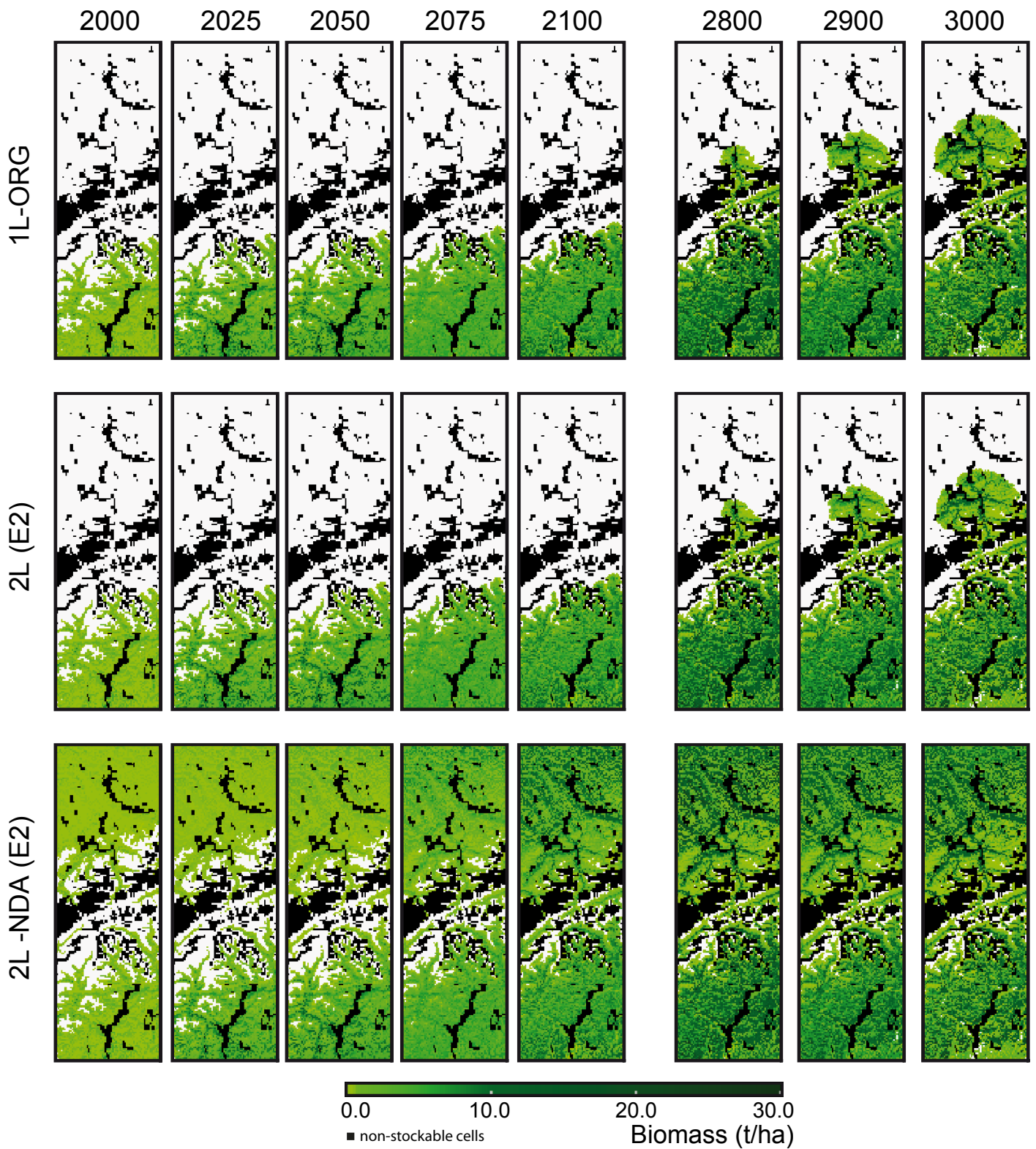
10

Fig. C.12: Maps of the biomass of *Ostrya carpinifolia* for different simulation years resulting in one-layer simulations with the original bioclimate driver (1L-ORG) and simulations with bioclimate types derived with the moderate set of bioclimate bins (E2 – Table 2, main text) and simulated with and without dynamic associations between cells on the two-dimensional layer and elements on the non-spatial layer (2L and 2L-NDA, respectively). Differences in the spatial spread of *O. carpinifolia* between 1L-ORG and 2L simulations on one side and the 2L-NDA simulation on the other side demonstrate the problem of simulations with a general availability of seeds for all species – as assumed in many dynamic vegetation models (see e.g. Snell et al., 2014) – and underline the importance to simulate migration explicitly. Maps of the biomass of *O. carpinifolia* were created with Paraview (Ahrens et al., 2005).

C.3. Sensitivity tests

In addition to the simulations discussed in the main text, several sensitivity tests were conducted using different splitting and merging thresholds, two different merging intervals and, for scenario A1, different numbers of tracked species.

C.3.1. Sensitivity tests for application scenario A1

For application scenario A1, each combination of the variants listed in Table C.2 was simulated with all three sets of bioclimate types (E1-E3) and with five different pseudo-random number streams used to extrapolate the bioclimate driver, i.e. 360 simulations were conducted.

Table C.2: Simulated variants of tracked species, splitting and merging thresholds and merging intervals.

Tracked species	**2**: *P. silvestris* and *Q. pubescens*	**4**[*]: The two and *O. carpinifolia* and *L. decidua*	**6**: The four and *P. abies* and *F. sylvatica*
Splitting thresholds	**1**: 0.05 germinated seeds per patch area	**2**[*]: 0.005 and 0.5 germinated seeds per patch area	
Merging accuracy	**c**[*]: Coarse merging thresholds[a]	**f**: Fine merging thresholds[b]	
Merging interval	**decade**	**century**[*]	

[*] Options used in the experiments in the main text.
[a] Similarity thresholds of 50.0, 25.0, 20.0, 15.0, 10.0, 7.5, 5.0, 2.5 individuals per patch for the lowest eight height classes, respectively, and 1.0 for all other height classes.
[b] Similarity thresholds of 5.0 individuals per patch area for the first seven height classes and 1.0 individuals for all other height classes.

The different combinations simulated for scenario A1 led to dramatic differences in the number of elements on the non-spatial layer over the simulated time span. The extremes of these combinations resulted in peak ratios of the number of elements compared to the number of cells in the simulation area from below 2% to around 70% (Fig. C.13). Despite the dramatic differences in the number of elements on the non-spatial layer over time, maximum differences in CPU time reductions were only around 12% (Fig. C.14). Largest differences in CPU time reductions were found among simulations with different number of tracked species when merging was conducted every century. The number of tracked species combined with the merging interval even had a stronger effect on CPU time reductions than the set of bioclimate types (E1-E3). In contrast to CPU time reductions, the level of SC_{spec} was mainly determined by the applied bioclimate types. In summary, simulations with application scenario A1 showed that the only notable increases in CPU time reductions were achieved by tracing less species or by shortening the merging interval from centuries to decades. Both changes slightly decreased the SC_{spec}, however, always depending on the other options selected.
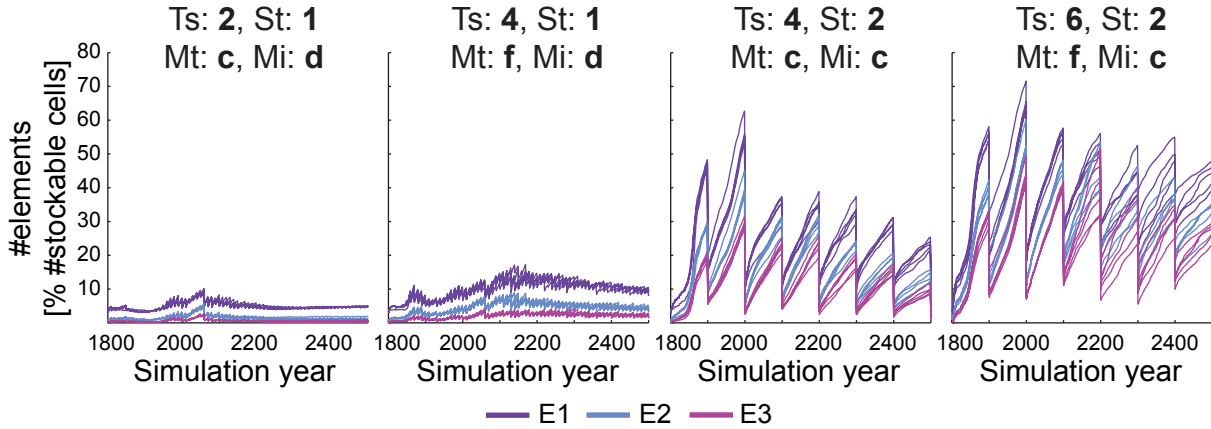

Fig. C.13: Temporal development of the elements on the non-spatial layer relative to the number of cells in the simulation area. Depicted are simulations using all three sets of bioclimate types (E1-E3) and different combinations of the options listed in Table C.2: tracked species (Ts), splitting thrsholds (St), merging accuracy (Ma) and merging intervals (Mi). On the left and on the right the extreme combinations are shown. On the left the 'coarsest': tracking absence and presence (St: 1) of two species (Ts: 2) and merging every decade (Mi: d) with coarse merging thresholds (Ma: c). On the right the 'finest': tracking six species (Ts: 6) with two splitting thresholds (St: 2) and merging every century (Mi: c) with finer merging thresholds (Ma: f). In the middle two moderate combinations are shown, of which the second is the combination used in the main text, namely tracking four species (Ts: 4) with two splitting thresholds (St: 2) and merging every century (Mi: c) with coarse merging thresholds (Ma: c). For CPU times and SC_{spec} values of these and other combinations see Fig. C.14.
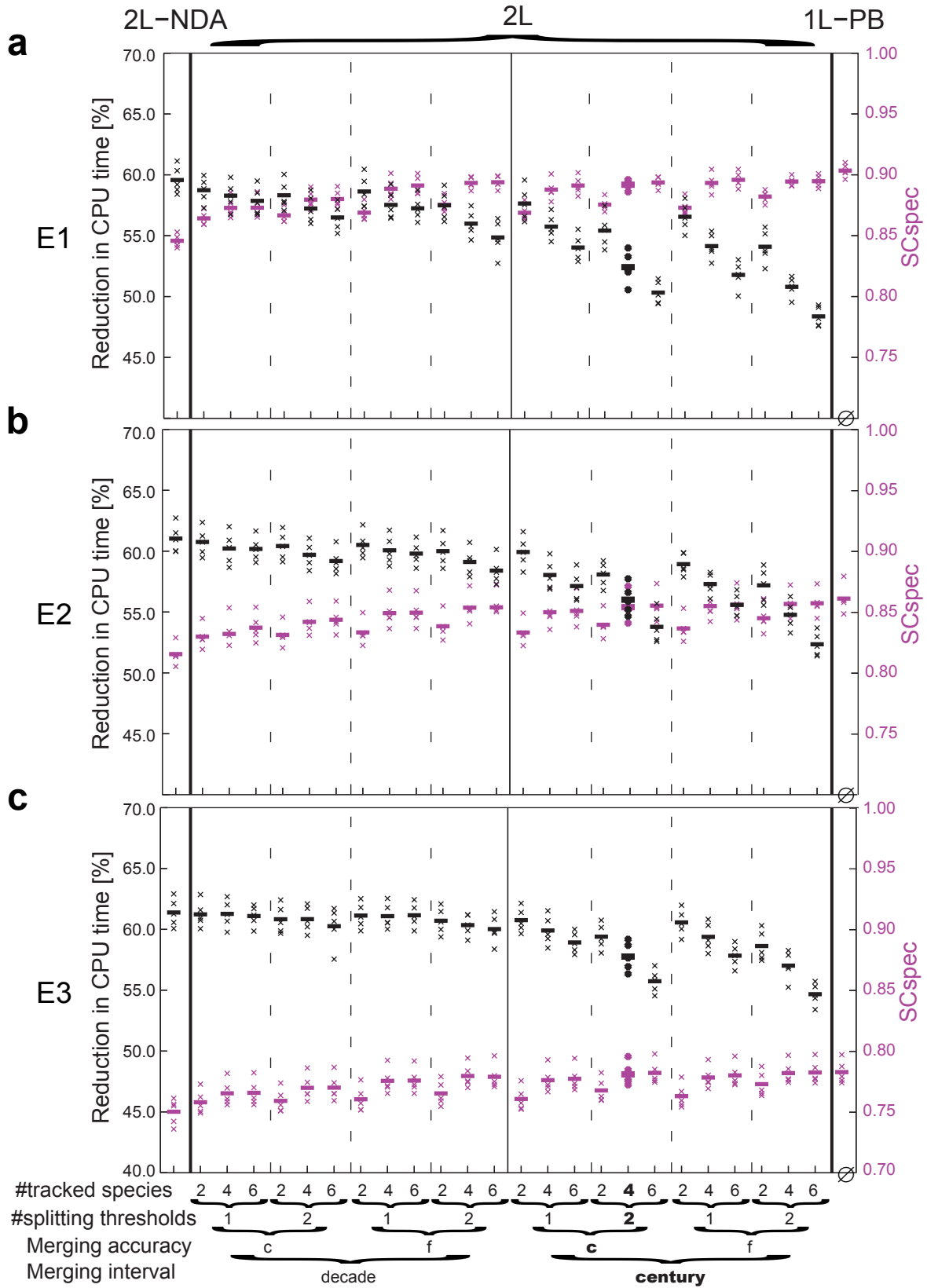
Fig. C.14: CPU time reductions and SC_{spec} values resulting from simulations of scenario A1 with each set of bioclimate types (E1-E3) using different splitting and merging settings (symbols on the x-axis are according to Table C.2). Additionally, CPU time reductions and SC_{spec} values resulting from two-layer simulations without dynamic associations (2L-NDA) and one-layer simulations with bioclimate types (1L-PB) are depicted. 1L-PB simulations did not led to reductions in CPU times (indicated by the empty set sign). Each simulation setting was repeated five times using different pseudo-random number streams to extrapolate the bioclimate driver. The CPU times for single simulations and the resulting SC_{spec} values in the last simulation year are depicted as crosses, the mean of the five simulations as a dash for each setting. The combination shown in the main text is depicted in bold.

13

C.3.2. Sensitivity tests for application scenario A2

For application scenario A2, the same splitting and merging threshold and the same merging intervals as for A1 were used (Table C.2). In addition, all combinations were simulated with a larger set of splitting thresholds (**6**: 0.0005, 0.005, 0.05, 0.5, 5.0 and 50.0 germinated seeds per patch area). Simulations were conducted using all three sets of bioclimate types (E1-E3) and 20 different pseudo-random number streams for the extrapolation of the bioclimate driver, i.e. in total 720 simulations were conducted.

Opposed to the large differences among A2 simulations with different bioclimate types, changes in other settings showed only tiny differences in the resulting mean CPU time reductions (maximum differences smaller than 3%) and the resulting mean SC_{spec} values (max differences smaller than 0.01 – Fig. C.15). The same was observed for most settings for mean SC_{OC} values (Fig. C.16), however, merging intervals of a decade in combination with the coarse merging thresholds led to stronger decreases in the mean SC_{OC} (maximum differences of about 0.08).
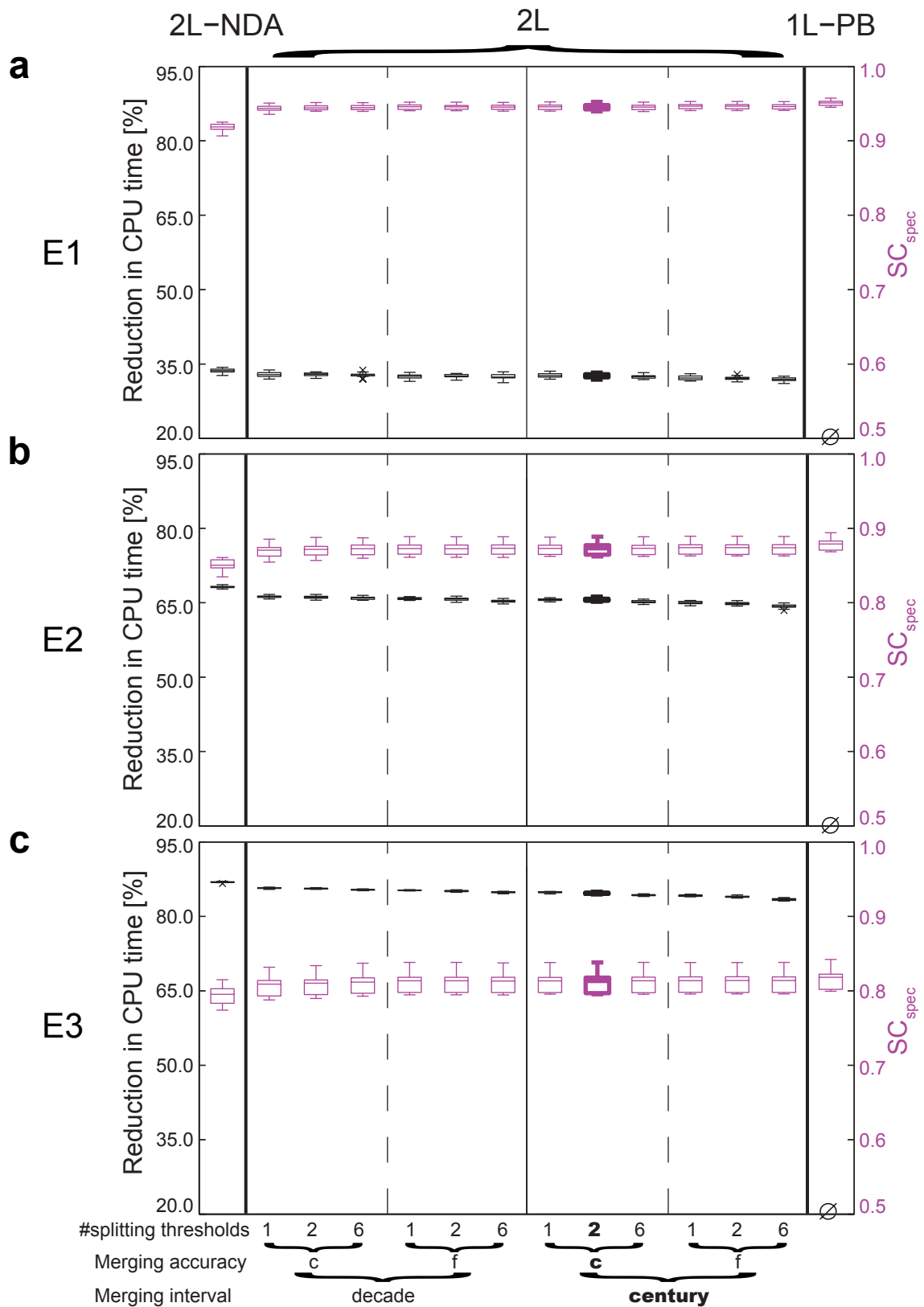
Fig. C.15: CPU time reductions and SC_{spec} values resulting from simulations of scenario A2 using different splitting and merging settings (symbols on the x-axis are according to Table C.2; for '6' splitting thresholds see text to Section C.3.2) and each of the three sets of bioclimate types (E1-E3). Additionally, CPU time reductions and SC_{spec} values resulting from two-layer simulations without dynamic associations (2L-NDA) and one-layer simulations with bioclimate types (1L-PB) are depicted. 1L-PB simulations did not led to reductions in CPU times (indicated by the empty set sign). Each simulation setting was repeated using 20 different pseudo-random number streams to extrapolate the bioclimate driver. The combination shown in the main text is depicted in bold.
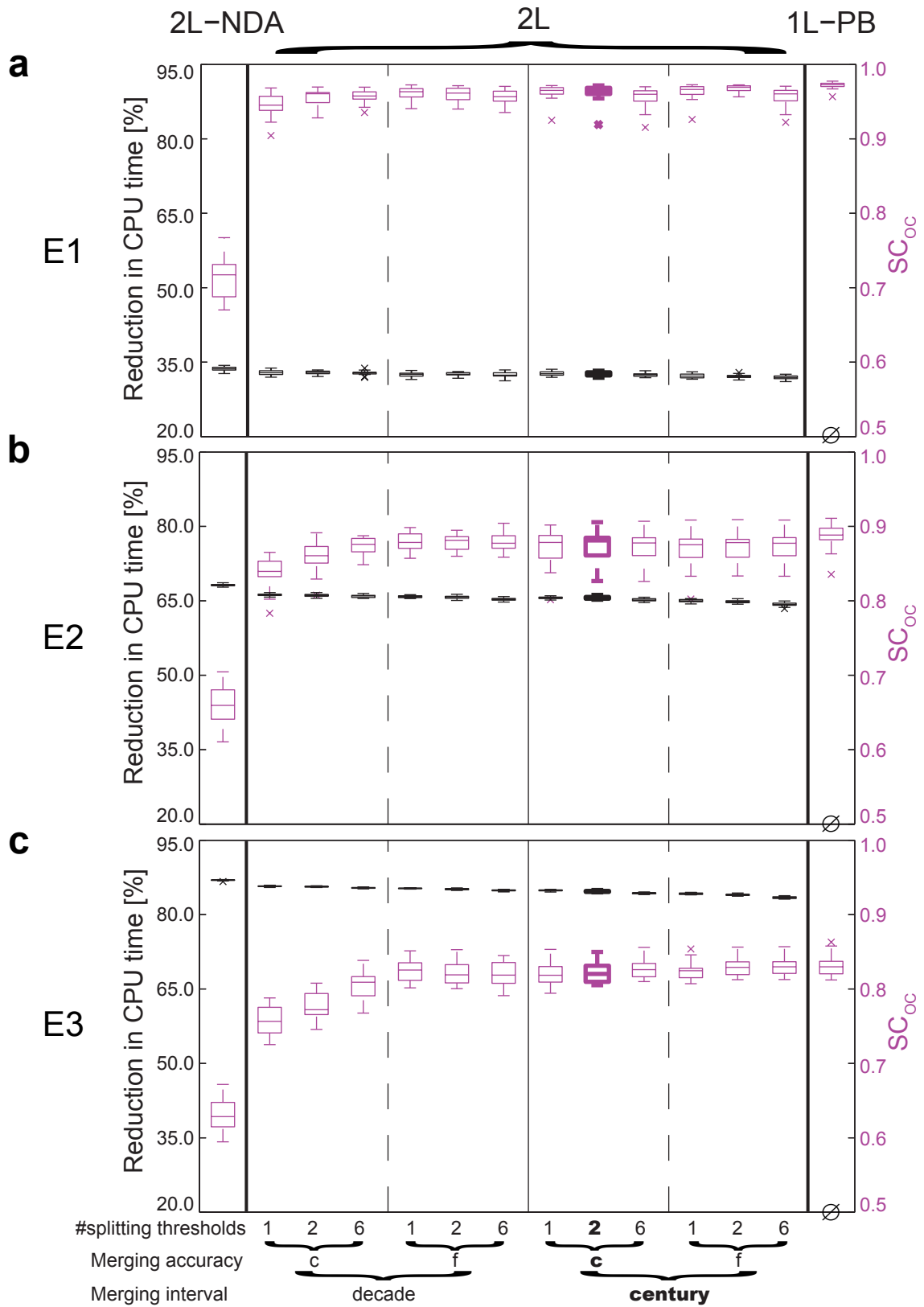
15

Fig. C.16: CPU time reductions and SC_{OC} values resulting from simulations of scenario A2 using different splitting and merging settings (symbols on the x-axis are according to Table C.2; for '6' splitting thresholds see text to Section C.3.2) and each of the three sets of bioclimate types (E1-E3). Additionally, CPU time reductions and SC_{OC} values resulting from two-layer simulations without dynamic associations (2L-NDA) and one-layer simulations with the bioclimate driver from the bioclimate types (1L-PB) are depicted. 1L-PB simulations did not led to reductions in CPU times (indicated by the empty set sign). Each simulation setting was repeated using 20 different pseudo-random number streams to extrapolate the bioclimate driver. The combination shown in the main text is depicted in bold.

16

References

Ahrens, J., Geveci, B., and Law, C.: Visualization Handbook, chap. ParaView: An End-User Tool for Large-Data Visualization, pp. 717–732, Elsevier Butterworth–Heinemann, Oxford, UK, 2005.

Bugmann, H.: On the Ecology of Mountainous Forests in a Changing Climate: A Simulation Study, Ph.D. thesis, Swiss Federal Institute of Technology Zurich, 1994.

Bugmann, H. and Cramer, W.: Improving the behaviour of forest gap models along drought gradients, Forest Ecology and Management, 103, 247–263, 1998.

Frei, E., Vökt, U., Flückiger, R., Brunner, H., and Schai, F.: Bodeneignungskarte der Schweiz auf Grund der Bodeneigenschaften ausgewählter physiographischer Landschaftselemente, Bundesämter für Raumplanung, Landwirtschaft und Forstwesen. Bern, 1980.

Hijmans, R. J., Cameron, S. E., Parra, J. L., Jones, P. G., and Jarvis, A.: Very high resolution interpolated climate surfaces for global land areas, International Journal of Climatology, 25, 1965–1978, 2005.

Kjellström, E., Bärring, L., Gollvik, S., Hansson, U., Jones, C., Samuelsson, P., Rummukainen, M., Ullerstig, A., U., W., and Wyser, K.: A 140-year simulation of European climate with the new version of the Rossby Centre regional atmospheric climate model (RCA3), SMHI Reports Meteorology and Climatology No. 108, SMHI, SE-60176, Norrkping, Sweden, 54 pp., 2005.

Klein, H.: FIMEX-0.28, https://wiki.met.no/fimex/start. Last access date: 09.01.12, 2012.

Lautenschlager, M., Keuler, K., Wunram, C., Keup-Thiel, E., Schubert, M., Will, A., Rockel, B., and Boehm, U.: Climate Simulation with CLM, Scenario A1B run no.1, Data Stream 3: European region MPI-M/MaD, World Data Center for Climate. http://dx.doi.org/10.1594/WDCC/CLM_A1B_1_D3, 2009.

Lischke, H., Löffler, T. J., and Fischlin, A.: Aggregation of Individual Trees and Patches in Forest Succession Models: Capturing Variability with Height Structured, Random, Spatial Distributions, Theoretical Population Biology, 54, 213–226, 1998.

Lischke, H., Zimmermann, N. E., Bolliger, J., Rickebusch, S., and Löffler, T. J.: TreeMig: A forest-landscape model for simulating spatio-temporal patterns from stand to landscape scale, Ecological Modelling, 199, 409–420, 2006.

Löffler, T. J. and Lischke, H.: Incorporation and influence of variability in an aggregated forest model, Natural Resource Modeling, 14, 103–137, 2001.

Mitchell, T., Carter, T., Jones, P., Hulme, M., and New, M.: A comprehensive set of climate scenarios for Europe and the globe, Tyndall centre Working paper 55, 2003.

Nabel, J. E. M. S. and Lischke, H.: Upscaling of spatially explicit and linked time and space discrete models studying vegetation dynamics under climate change, In: B. Page, A.G. Fleischer, J. Gbel, V. Wohlgemuth (Eds.) (2013): Environmental Informatics and Renewable Energies - 27th International Conference on Informatics for Environmental Protection. Shaker Verlag, Germany, pp. 842-850, ISBN 978-3-8440-1676-5, http://enviroinfo.eu/sites/default/files/pdfs/vol7995/0842.pdf. Last access date: 19.06.15, 2013.

Nabel, J. E. M. S., Zurbriggen, N., and Lischke, H.: Impact of species parameter uncertainty in simulations of tree species migration with a spatially linked dynamic model., In: R. Seppelt, A.A. Voinov, S. Lange, D. Bankamp (Eds.) (2012): International Environmental Modelling and Software Society (iEMSs) 2012. Managing Resources of a Limited Planet: Pathways and Visions under Uncertainty, Sixth Biennial Meeting, Leipzig, Germany. p.909-916. ISBN: 978-88-9035-742-8, http://www.iemss.org/society/index.php/iemss-2012-proceedings, Last access date: 30.04.15, 2012.

Nabel, J. E. M. S., Zurbriggen, N., and Lischke, H.: Interannual climate variability and population density thresholds can have a substantial impact on simulated tree species' migration, Ecological Modelling, 257, 88–100, 2013.

Nabel, J. E. M. S., Kirchner, J. W., Zurbriggen, N., Kienast, F., and Lischke, H.: Extrapolation methods for climate time series revisited – Spatial correlations in climatic fluctuations influence simulated tree species abundance and migration, Ecological Complexity, 20, 315–324, 2014.

Nakicenovic, N., Alcamo, J., Davis, G., de Vries, B., Fenhann, J., Gaffin, S., Gregory, K., Grübler, A., Jung, T. Y., Kram, T., La Rovere, E. L., Michaelis, L., Mori, S., Morita, T., Pepper, W., Pitcher, H., Price, L., Riahi, K., Roehrl, A., Rogner, H. H., Sankovski, A., Schlesinger, M., Shukla, P., Smith, S., Swart, R., van Rooijen, S., Victor, N., and Dadi, Z.: IPCC Special Report on Emissions Scenarios, Cambridge University Press, UK, 2000.

Pierce, D.: Ncview-1.93g, http://meteora.ucsd.edu/~pierce/ncview_home_page.html. Last access date: 14.07.12, 2012.

Rickebusch, S., Lischke, H., Bugmann, H., Guisan, A., and Zimmermann, N. E.: Understanding the low-temperature limitations to forest growth through calibration of a forest dynamics model with tree-ring data, Forest Ecology and Management, 246, 251–263, 2007.

Snell, R. S., Huth, A., Nabel, J. E. M. S., Bocedi, G., Travis, J. M. J., Gravel, D., Bugmann, H., Gutiérrez, A. G., Hickler, T., Higgins, S. I., Scherstjanoi, M., Reineking, B., Zurbriggen, N., and Lischke, H.: Using individual based forest models to simulate species range shifts, Ecography, 37, 1184–1197, 2014.

Thornton, P. E., Running, S. W., and White, M. A.: Generating surfaces of daily meteorological variables over large regions of complex terrain, Journal of Hydrology, 190, 214–251, 1997.